VCSELs for Atomic Sensors

D. K. Serkland*[a], K. M. Geib[a], G. M. Peake[a], R. Lutwak[b], A. Rashed[b],
M. Varghese[c], G. Tepolt[c], M. Prouty[d]

[a]Sandia National Laboratories, Albuquerque, NM 87185
[b]Symmetricom, Inc., Beverly, MA 01915
[c]Charles Stark Draper Laboratory, Cambridge, MA 02139
[d]Geometrics, Inc., San Jose, CA 95131

ABSTRACT

A new generation of small low-power atomic sensors, including clocks, magnetometers, and gyroscopes, is being developed based on recently available MEMS and VCSEL technologies. These sensors rely on spectroscopic interrogation of alkali atoms, typically rubidium or cesium, contained in small vapor cells. The relevant spectroscopic wavelengths (in vacuum) are 894.6 nm (D1) and 852.3 nm (D2) for cesium, and 795.0 nm (D1) and 780.2 nm (D2) for rubidium. The D1 wavelengths are either preferred or required, depending on the application, and vertical-cavity surface-emitting lasers (VCSELs) are preferred optical sources because of their low power consumption and circular output beam.

This paper describes the required VCSEL characteristics for atomic clocks and magnetometers. The fundamental VCSEL requirement is single-frequency output with tunability to the particular spectroscopic line of interest. Single-polarization and single-transverse-mode operation are implicit requirements. VCSEL amplitude noise and frequency noise are also important because they contribute significantly to the sensor signal-to-noise ratio. Additional desired VCSEL attributes are low cost, low power consumption, and several years of continuous operating lifetime.

This paper also describes the 894-nm VCSELs that we have developed for cesium-based atomic sensors. In particular, we discuss VCSEL noise measurements and accelerated lifetime testing. Finally, we report the performance of prototype atomic clocks employing VCSELs.

Keywords: VCSEL, vertical-cavity surface-emitting laser, atomic clock, magnetometer, gyroscope, spectroscopy, cesium, rubidium, linewidth, relative intensity noise, frequency standard

1. INTRODUCTION

In 2002, the Defense Advanced Research Projects Agency (DARPA) initiated a program to develop a Chip-Scale Atomic Clock (CSAC), which would enable high-accuracy timing in portable battery-powered devices. In particular, DARPA set a 4-year goal to produce a prototype atomic clock having volume < 1 cm^3, power consumption < 30 mW, and fractional frequency instability (Allan deviation) < $1x10^{-11}$ over a 1-hour averaging interval. Such portable atomic clocks could be carried into locations where reception of Global Positioning System (GPS) signals is impaired and enable position information to be quickly and accurately determined by using the timing information from the atomic clock rather than from the GPS satellites. Moreover, if such clocks could be mass produced using micro-electronics fabrication techniques, the unit cost could be reduced to the point where such clocks could replace ovenized crystal oscillators in a large number of precision timing applications.

In 2000, the demonstration of an all-optical atomic clock using a modulated VCSEL[1] rather than an RF cavity paved the way to dramatically reduce the size and power consumption of atomic frequency standards. This paper will discuss the requirements of VCSELs used in atomic clocks. Since atomic clocks have relatively demanding requirements on VCSELs, compared to data communication applications, it is expected that such high-precision VCSELs will be more costly to produce. In the long run, the growth of the market will depend largely on the ability of the VCSEL manufacturers to reduce the cost of this critical component.

*DKSERKL@sandia.gov; phone: (505) 844-5355; fax: (505) 844-8985; http://www.sandia.gov

Similar to atomic clocks, atomic magnetometers and gyroscopes can benefit by replacing the traditional gas discharge lamp light source with a VCSEL to reduce the sensor power consumption by more than 5 W. The existing market for high-precision atomic magnetometers is approximately an order of magnitude smaller than that of atomic clocks. However, due to their higher cost, atomic magnetometers could tolerate more expensive VCSELs, and thereby provide additional incentive for commercialization of VCSELs for atomic sensors. While atomic gyroscopes have demonstrated navigational grade performance in the laboratory, they are not currently available as commercial products. Atomic gyroscopes will not specifically be discussed in this paper, but we note that their demands on VCSELs are most similar to atomic magnetometers.

2. ATOMIC SENSOR PHYSICS

In this section we will discuss the essential physics of atomic clocks and magnetometers, with the goal of understanding the basis of the VCSEL requirements to be discussed in the following section.

2.1. Atomic clock physics

Previous publications have described the optical-microwave double resonance interrogation technique employed in conventional rubidium atomic clocks.[2,3] Here we review the all-optical coherent population trapping (CPT) technique that enables smaller and lower-power atomic clocks using VCSELs.

Coherent population trapping (CPT) offers an all-optical interrogation method that does not require an RF cavity surrounding the alkali gas cell.[4] Fig. 1(a) shows the relevant energy levels of the valence electron in a cesium (Cs) atom. Similar to rubidium, the $6S_{1/2}$ ground state of Cs is split into 2 sublevels, labeled a and b, due to the hyperfine interaction between the nuclear and electronic spins. The hyperfine splitting of the ground state of Cs is approximately 9.2 GHz. In fact, the internationally-accepted definition of the second is 9,192,631,770 oscillation periods of the cesium hyperfine frequency. Coherent population trapping requires the simultaneous application of 2 coherent optical frequencies f_{ac} and f_{bc}, such that the difference frequency exactly equals the 9.2 GHz ground state hyperfine splitting. A clever and convenient way to obtain 2 such frequencies is to modulate a VCSEL at 4.6 GHz with a small-amplitude sinusoidal waveform, thereby obtaining coherent frequency modulation (FM) sidebands at ±4.6 GHz from the carrier optical frequency of 352 THz (852nm), as shown schematically in Fig. 1(c). Fig. 1(b) shows the required elements of a CPT atomic clock; namely, a 4.6 GHz microwave source to drive the VCSEL with approximately 0 dBm of power, a VCSEL with > 4 GHz FM modulation bandwidth tuned to exactly 852.4 nm (vacuum wavelength), a quarter-wave plate to create a pure circular polarization state, a cesium cell heated to approximately 80°C, and an audio-bandwidth photodiode (PD) to measure transmission of the VCSEL light. If the 4.6 GHz FM modulated VCSEL is tuned by increasing its DC drive current, the transmitted optical power measured by the photodiode exhibits a 1-GHz-wide absorption dip, shown in Fig. 1(d), when the laser is tuned to the mid-point between the f_{ac} and f_{bc} frequencies, such that the first-order sidebands excite both the f_{ac} and f_{bc} transitions simultaneously.

Coherent population trapping (CPT) refers to the fact that a fraction of the cesium atoms become “trapped” in a coherent superposition of the ground states a and b, which does not absorb light due to destructive interference between the ac and bc transition probability amplitudes.[5,6] When the modulated VCSEL is tuned to the approximately 1 GHz-wide absorption resonance, and the modulation frequency is tuned in the vicinity of 4.6 GHz, a narrow (and small) increase in the transmitted optical power is observed at exactly half of the 9.2 GHz hyperfine frequency, as shown schematically in Fig. 2. In an atomic clock application, the 4.6 GHz microwave source is locked to this narrow CPT resonance, yielding a frequency that is exactly half of the cesium ground state hyperfine splitting. A CPT frequency standard can also be made using rubidium (instead of cesium), in which case the microwave frequency is locked to the rubidium CPT resonance at ½(6.8 GHz)=3.4 GHz.

For either Cs or Rb, there are two possible optically excited states “c” that can be employed, due to the fine structure (spin-orbit) splitting of the upper P-state. The two possible optical absorption wavelengths are designated D1 and D2,

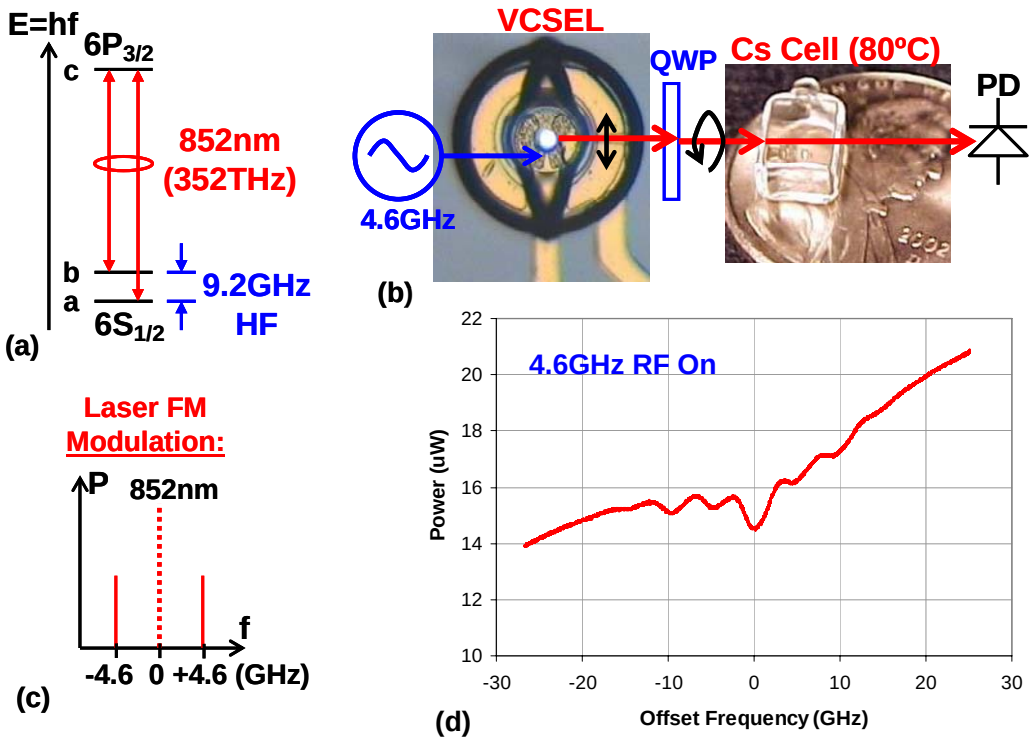

Fig. 1. Coherent population trapping (CPT) atomic clock physics. (a) Cesium energy levels, showing the ground state 9.2-GHz hyperfine level splitting and the optical 852-nm D2 transition. (b) Schematic of a typical CPT atomic clock. (c) Illustration of the first order sidebands at ±4.6 GHz created by frequency modulation of the VCSEL. (d) Detected power of the modulated VCSEL versus frequency offset. The VCSEL frequency was tuned over this small 50-GHz range by increasing its DC drive current by a small amount (0.4 mA).

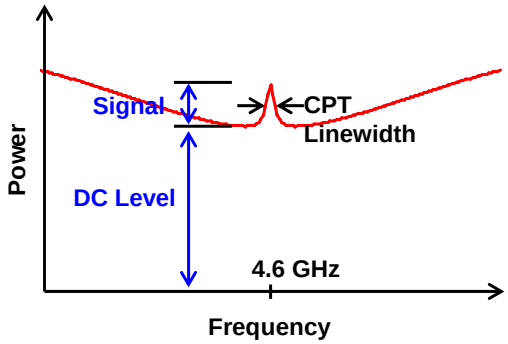

Fig. 2. Schematic illustration of the CPT resonance peak versus the RF frequency driving the VCSEL. The contrast is defined as η = Signal/(DC Level). The figure of merit is defined as ξ=ηQ, where Q is the ratio of the RF resonance frequency to the CPT linewidth. Typically the contrast is on the order of 1% and the linewidth is on the order of 1 kHz.

corresponding to the $P_{1/2}$ and $P_{3/2}$ excited states, respectively. For cesium, the D1 transition occurs at 894.6 nm (vacuum wavelength) and the D2 transition occurs at 852.4 nm (vacuum wavelength). For rubidium, the D1 line is at 795.0 nm (vacuum wavelength) and the D2 line is at 780.2 nm (vacuum wavelength). For both rubidium[7] and cesium[8] it has been demonstrated that the CPT clock resonance figure of merit, defined in Fig. 2, is higher for the D1 transition. For this reason, the D1 wavelength is generally preferred over the D2 wavelength for atomic clocks.

2.2. Atomic magnetometer physics

An atomic magnetometer consists of components nearly identical to the atomic clock discussed above, with the notable difference that no microwave modulation of the VCSEL is needed for the magnetometer. Of several possible configurations, the Mx magnetometer, shown schematically in Fig. 3(a), is one of the most popular.[9,10] The Mx magnetometer is made to self-oscillate at the Larmor frequency (f_L) by amplifying the photodiode output and feeding this signal back (with a 90-degree phase shift) to the H_1 coil. The typical 50,000 nT magnitude of Earth's magnetic field yields a Larmor frequency of 175 kHz, which is determined by the Zeeman splitting of the cesium ground state energy levels shown in Fig. 3(b). In this manner, the oscillation frequency is directly proportional to the magnitude of the DC magnetic field H_0 to be sensed – it is a scalar (not a vector) magnetometer. The Mx magnetometer is named for the fact that if the z-axis is taken along the direction of H_0, then the precession of the atomic magnetic moment **M** about z yields a maximum intensity modulation of circularly polarized sense light directed along the x axis (detecting the oscillating Mx component of the magnetic moment). The Mx magnetometer typically employs a single circularly polarized light beam both to pump the atoms into a spin-polarized state and to detect the magnetic moment Mx that oscillates at the Larmor frequency. The Mx magnetometer configuration has "dead zones" of zero sensitivity when it is oriented at 0° or 90° relative to the sensed magnetic field H_0.[9]

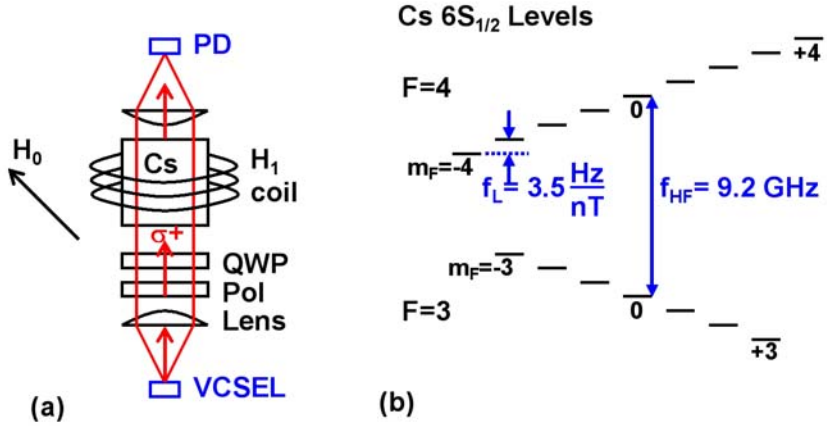

Fig. 3. (a) Schematic drawing of a cesium Mx magnetometer used to sense the ambient magnetic field H_0. (b) Cesium $6S_{1/2}$ ground state energy levels, illustrating the Zeeman splitting of the F=3 and F=4 states in a magnetic field H_0.

3. VCSEL REQUIREMENTS FOR ATOMIC SENSORS

In this section we will describe the requirements for VCSELs to be used in atomic sensors, as motivated by the physics discussed in the previous section.

First, the VCSEL must operate at a single frequency that is tunable to exactly the D1 or D2 resonance wavelength of Cs or Rb. The relevant optical transition wavelengths (in vacuum) are for cesium 894.6 nm (D1) and 852.4 nm (D2), and for rubidium 795.0 nm (D1) and 780.2 nm (D2). The D1 transition wavelengths are generally preferred because they yield higher performance.[7,8] In order to stabilize the VCSEL wavelength to within the Doppler-broadened atomic linewidth, its temperature must be stabilized to within 10 millidegrees centigrade. If active cooling of the VCSEL is not possible, the operating temperature of the VCSEL must be chosen above the maximum ambient temperature at which the atomic sensor is specified to operate. For example, if an atomic clock is specified to operate from 0 to 70°C, then the operating temperature of the VCSEL might be chosen at nominally 85°C. If the VCSEL temperature can only be varied within a ±5°C range, then the VCSEL wavelength must be accurate to within ±0.3 nm (assuming a typical VCSEL tuning coefficient of 0.06 nm/°C). Moreover, the VCSEL must operate in a single linear polarization so that a quarter-wave plate (QWP) can be used to produce a pure circular polarization in the alkali-atom gas cell. Circular polarization is required to enforce selection rules on the optical transitions (an explanation of the selection rules can be found in the references cited in the previous section). Perhaps most importantly, the VCSEL must operate at this

precise wavelength in a stable single frequency and polarization mode for the life of the instrument, typically 10 years or longer.

The requirements for linear polarization, single frequency, and precise output wavelength at the prescribed operating temperature have significant implications for VCSEL device yield. In order to have a VCSEL yield above 90%, the typical example discussed above would require an epitaxial growth accuracy of ±0.15 nm and uniformity across the 3-inch GaAs wafer of ±0.15 nm. These requirements are approximately 10 times more demanding than typical accuracies obtained in the best epitaxial growth facilities. In addition, for oxide confined VCSELs, the oxide aperture diameter (typically about 3 μm for single transverse mode operation) must be controlled to within ±0.1 μm, since the wavelength also depends on the oxide aperture diameter. This requirement is approximately 2 times more demanding than the results that are achieved at the most reproducible fabrication facilities. Thus, it seems likely that production yields of VCSELs that meet the atomic sensor wavelength requirements might be 10% or less, even with exceptionally accurate epitaxial growth and fabrication.

For low power consumption of atomic sensors, the VCSEL DC power consumption should be limited to 2 mW, which necessitates a threshold current below 1 mA. For most oxide-confined VCSELs this threshold current requirement is not difficult to meet. In order to create FM sidebands (at for example ±4.6 GHz), the VCSEL should have an FM modulation bandwidth above 4 GHz. This requirement is also motivated by the desire for low power consumption of the atomic clock, since ideally 0 dBm (1 mW) of RF power at 4.6 GHz should be sufficient to transfer most of the carrier frequency power into the sidebands at ±4.6 GHz. A key ingredient that enables efficient RF frequency modulation of the VCSEL is impedance matching of the VCSEL to the driving RF oscillator.

Ultimately, if other noise sources are eliminated, the signal-to-noise ratio of an atomic sensor is limited by the intensity noise on the detected photocurrent. Relative intensity noise (RIN) of the VCSEL should therefore be reduced toward the shot noise level within the 1 to 300 kHz range of detection frequencies employed for atomic clocks and magnetometers. In particular, VCSELs are known to exhibit significant 1/f noise with corner frequencies ranging from 1 to 100 kHz. Fig. 4 shows the RIN of an 852-nm VCSEL designed for atomic clocks. In the case of atomic clocks, the VCSEL output is typically attenuated to avoid systematic frequency offsets due to high optical intensities. Optical attenuation of a laser has the beneficial effect of lowering excess intensity noise toward the shot noise level. Due to the requirement to optically polarize the atoms in a magnetometer, little or no attenuation may be desired in that application.

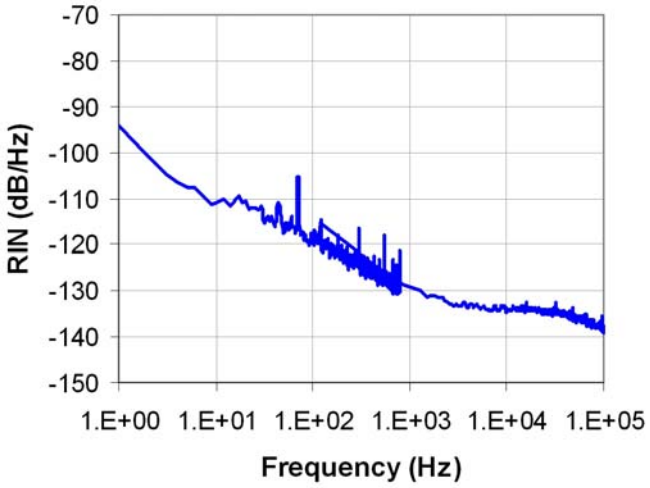

Fig. 4. Relative intensity noise (RIN) of an 852-nm VCSEL versus frequency, showing a 1/f corner frequency near 2 kHz.

The final VCSEL requirement that we will discuss is the desire for a narrow linewidth (< 100 MHz). To understand the impact of VCSEL linewidth on sensor performance, consider a VCSEL that is tuned to the center of the 1-GHz-wide absorption dip shown in Fig. 1(d). Any frequency noise present on the laser will be converted to amplitude noise due to

the slope of the atomic transmission versus frequency curve, as shown schematically in Fig. 5(a), and thus is indistinguishable from other noise sources (such as RIN or atomic shot noise) on the detected signal. In order to minimize amplitude noise on the transmitted optical signal, the laser linewidth (measured in a bandwidth comparable to the loop bandwidth of the atomic clock) should be less than 10% of the approximately 1-GHz-wide absorption dip. Due to the inherently short photon lifetime in a typical VCSEL cavity, achieving < 100 MHz linewidth is challenging. A typical VCSEL has a linewidth of a few hundred MHz, and the narrowest reported VCSEL linewidth is approximately 3 MHz.[11] It should also be mentioned that due to the strong dependence of VCSEL frequency on drive current (typically -125 MHz/μA), the current source that drives the VCSEL must be very stable to achieve a narrow linewidth. Fig. 5(b) shows the measured linewidth of an 852-nm VCSEL designed for atomic clocks.[3]

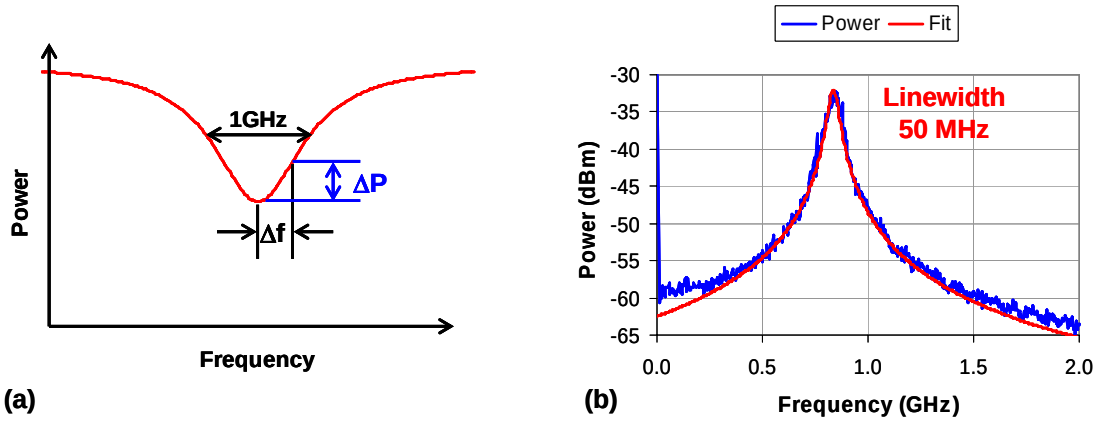

Fig. 5. (a) Schematic illustration of the conversion of laser frequency noise to transmitted amplitude noise by the approximately 1-GHz-wide absorption line shape. (b) Measured clock-VCSEL linewidth data, which is fit well by a 50-MHz-wide Lorentzian.

4. MINIATURE ATOMIC CLOCKS USING 894-NM VCSELS

In phase 3 of DARPA's CSAC program, the Symmetricom-Draper-Sandia team was tasked to produce 10 prototype CSACs, each having a volume of 16 cm^3 and a power consumption of 125 mW. In order to reduce production cost relative to the phase 2 CSAC prototype,[12] the VCSEL chip size was reduced from 2-mm square to 0.5-mm square, as shown in Fig. 6(a). The result was that 16 times the number of VCSEL chips were obtained from each 3-inch GaAs wafer, and thus the cost of the VCSEL component was reduced 16-fold. Fig. 6(b) shows an optical micrograph of a phase-3 VCSEL chip with one of the VCSELs illuminated.

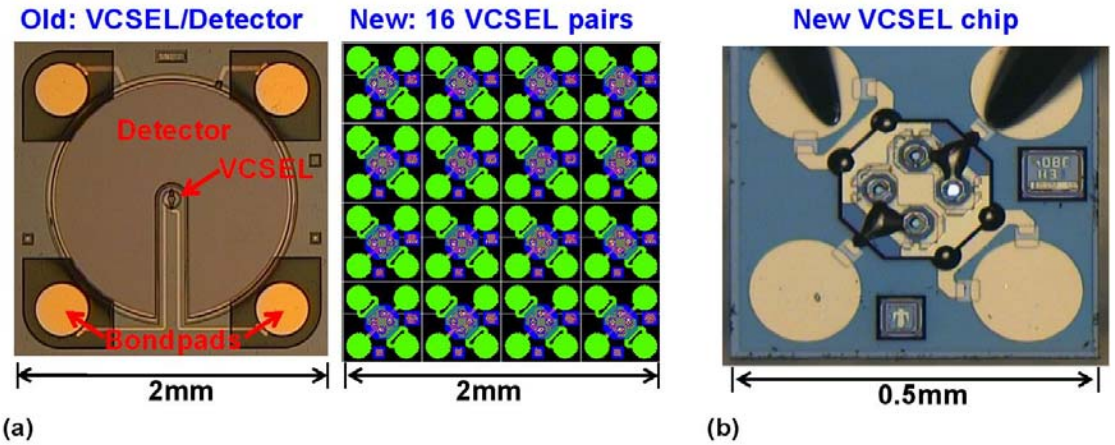

Fig. 6. (a) Phase-2 VCSEL/Detector chip occupies the same GaAs wafer area as 16 phase-3 VCSEL chips. (b) Optical micrograph of the 0.5-mm-square phase-3 VCSEL chip, with 1 of 2 VCSELs illuminated.

The optical path inside the physics package was changed from the double-pass configuration, shown in Fig. 7(a), to a single-pass configuration. A silicon photodiode chip, having dimensions nominally identical to the phase 2 VCSEL/detector chip, was placed on the opposite side of the cesium cell from the VCSEL. The physics package, fabricated at Draper Laboratory, retained essentially the same configuration and size that was employed in phase 2, as shown by the photograph in Fig. 7(b).

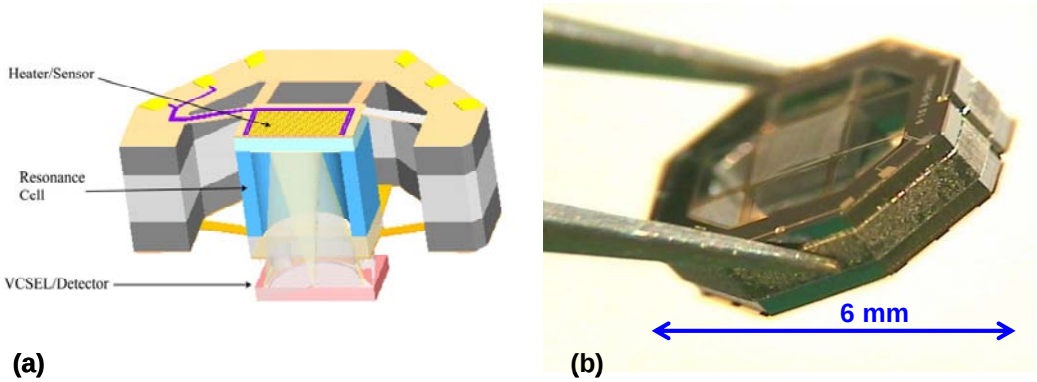

Fig. 7. (a) Cross sectional schematic drawing of phase-2 physics package. (b) Picture of a fabricated cell suspension.

As in phase 2, the epitaxial semiconductor structure of the 894-nm VCSELs was grown on a semi-insulating GaAs substrate to minimize parasitic capacitances. The bottom distributed Bragg reflector (DBR) was designed as a high reflector, containing 36 pairs of n-doped quarter-wave high-index $Al_{0.16}Ga_{0.84}As$ and low-index $Al_{0.92}Ga_{0.08}As$ layers. The active region contained 5 undoped (intrinsic) $In_{0.07}Ga_{0.93}As$ quantum wells to provide optical gain near 890 nm. A quarter-wave layer of p-doped $Al_{0.98}Ga_{0.02}As$ immediately above the active region was selectively oxidized to form a circular oxide aperture that confined current to the center of the device.[13] The oxide aperture diameter was kept below 4 microns so that the VCSEL emitted predominantly in the fundamental transverse mode.[14] The top DBR was designed as an output coupling mirror, containing 21 pairs of p-doped quarter-wave low-index and high-index layers. A thin layer of metal was deposited over the VCSEL aperture to attenuate the optical output power by 13-dB, thereby limiting the optical power at the cell to near the optimum level of 0.02 mW. The output power and voltage versus current data for a 3-micron-aperture VCSEL are shown in Fig. 8(a). Notice that the threshold is only 0.3 mA at 1.46 V, so that less than 1 mW of DC electrical power is required to operate the VCSEL. The VCSEL is optimized for single longitudinal and transverse mode operation with a linearly polarized output. The optical emission spectrum of the VCSEL at a drive current of 3.0 mA is shown in Fig. 8(b). The spectrum shows that the higher order transverse modes are suppressed by approximately 33 dB relative to the fundamental transverse mode.

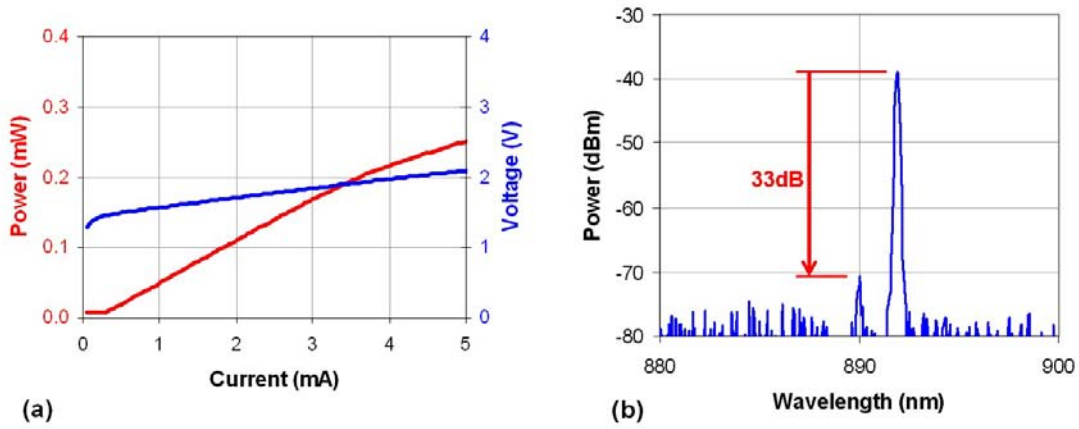

Fig. 8. (a) VCSEL output power and voltage versus current. The threshold current is 0.3 mA and the threshold voltage is 1.46 V. (b) VCSEL emission spectrum at 3 mA, showing approximately 33 dB suppression of higher order transverse modes.

Fig. 9(a) schematically shows how the physics package from Fig. 7(a) was mounted on a 35 mm by 39 mm printed circuit board containing all of the atomic clock circuitry, including the 4.6-GHz microwave oscillator.[12] The fully packaged CSAC prototype is shown in Fig. 9(b), mounted on an evaluation PCB for testing. The fully-packaged prototype enclosed a volume of 16 cm^3, and the operating power of the atomic clock was 125 mW.

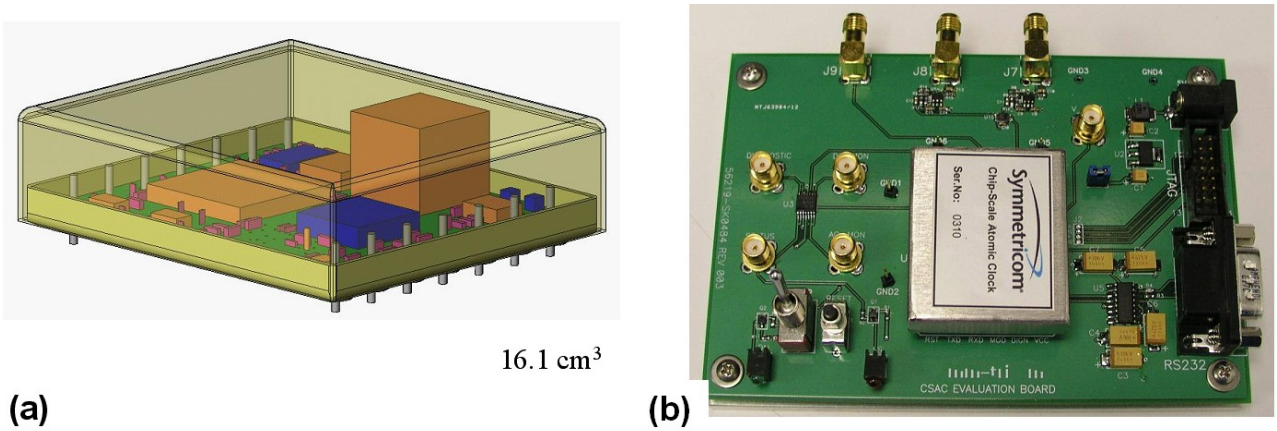

Fig. 9. (a) Schematic of CSAC prototype printed circuit board containing the physics package (tall cube), a 4.6-GHz voltage controlled oscillator, a phase locked loop, and microprocessor for controlling the cell temperature, the VCSEL current, and the oscillator frequency. (b) The fully packaged prototype CSAC having volume less than 16 cm^3 and mounted on a demonstration printed circuit board.

Fig. 10 shows the Allan deviation of the relative offset frequency $y = (f_{meas} - f_0)/f_0$ versus the measurement time interval τ, for a typical CSAC prototype. The short term frequency stability is near $\sigma_y = 2 \times 10^{-10}/\tau^{1/2}$, which surpasses the DARPA specification of $\sigma_y = 6 \times 10^{-10}/\tau^{1/2}$.

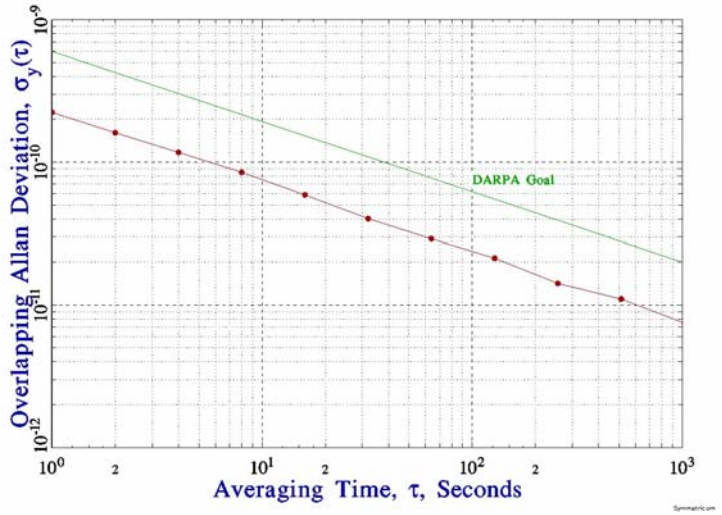

Fig. 10. Allan deviation of the CSAC prototype offset frequency $y = (f_{meas} - f_0)/f_0$ versus averaging time, showing that the prototype readily exceeds the DARPA performance goal.

Finally we consider long-term reliability of the VCSELs, which will likely determine the operating lifetime of an atomic clock. We note that if no thermoelectric cooler is employed, the VCSEL must operate at a temperature somewhat above the maximum ambient temperature. It is well known that elevated temperatures accelerate VCSEL aging by a factor of

2 for every 10°C increase in operating temperature.[15] The other factor that accelerates VCSEL aging is current density.[15] The relatively small apertures employed for single mode operation tend to increase current density. Fortunately, because very little output power is required, the VCSEL can be operated satisfactorily at current levels below 2 mA. Based on aging data published previously by Honeywell (now Finisar, Advanced Optical Components),[16] we estimate a MTTF of approximately 10 years for a 3.5-micron-aperture VCSEL operating at 1.5 mA at 85°C. In order to verify this lifetime estimate, we subjected 23 of our 894-nm clock VCSELs to accelerated aging conditions (current densities of 25 kA/cm^2 at an ambient temperature of 90°C), which yields an acceleration factor greater than 10. Fig. 11 shows the optical power of 16 of the 23 VCSELs that were monitored for 8 months. At the end of 8 months, 8 of these 16 VCSELs had failed (>20% drop in output power). Of the 8 failures, 6 devices had apertures >= 5.0 microns, which required higher current levels to achieve a current density of 25 kA/cm^2, and thus these devices heated up more than the smaller-aperture VCSELs yielding acceleration factors much higher than 10. Although we have not yet carefully analyzed our lifetime data, the results immediately support a MTTF on the order of 10 times 8 months, which is over 6 years. Also, it should be noted that our lifetime estimate is pessimistic in that it is based on old data and newer device designs and fabrication techniques generally improve device reliability.

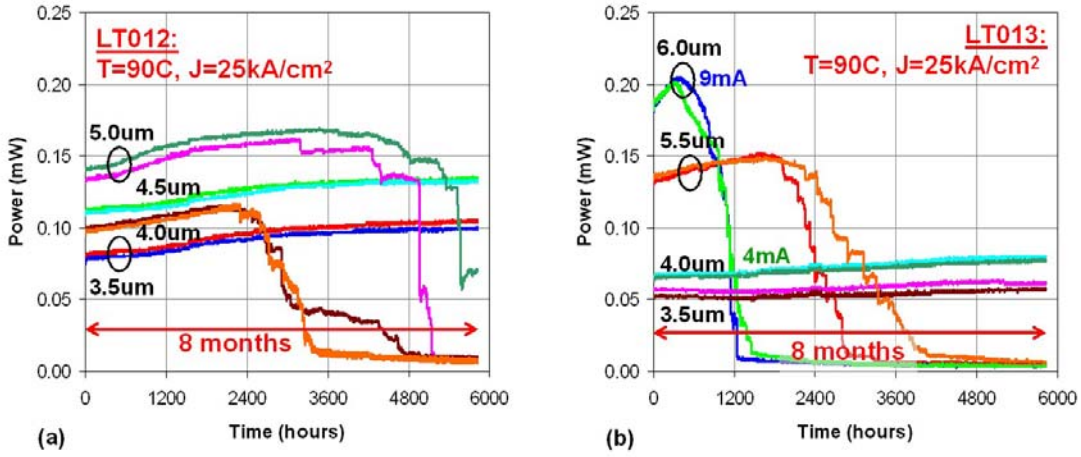

Fig. 11. Accelerated aging data from 16 VCSELs operated at current densities of 25 kA/cm^2 and at an ambient temperature of 90°C for 8 months. Half of these VCSELs failed within 8 months.

5. CONCLUSIONS

In conclusion, high performance atomic sensors based on alkali vapor cells can reduce power consumption by over 50% simply by replacing the gas discharge lamp with a VCSEL light source. Additional power savings achieved with smaller alkali vapor cells can yield 2 orders of magnitude total reduction in power consumption, thereby enabling new applications for atomic sensors. VCSELs are preferred optical sources due to their low power consumption, circular output beam, and high modulation bandwidth. The VCSEL must operate in a single frequency mode that is tunable to the atomic transition wavelength, preferably the rubidium D1 transition at 795.0 nm or the cesium D1 transition at 894.6 nm. This rigid wavelength constraint will likely result in a significant loss of yield during VCSEL production.

Other VCSEL requirements for atomic sensors include linearly polarized output, narrow linewidth (< 100 MHz), low power consumption (< 2 mW), high frequency modulation bandwidth (> 4 GHz), and impedance matching to the driving RF oscillator at 3.4 GHz (Rb) or 4.6 GHz (Cs). Achieving a narrow VCSEL linewidth is typically one of the more important challenges for optimum atomic sensor performance. While the potential market for atomic clock VCSELs will probably not exceed 100,000 devices/year within the next 5 years, we believe that the market can support a high-volume VCSEL cost approximately 10 times that of a standard data communication VCSEL.

ACKNOWLEDGEMENT

The authors wish to thank G. A. Keeler, T. M. Bauer, J. Nagyvary, V. M. Montaño, and I. C. Reines for their expert technical assistance. They also thank R. M. Garvey, K. Smith, P. D. D. Schwindt, S. Knappe, and J. Kitching for valuable discussions. The atomic clock work was supported by DARPA, at Sandia under MIPR number 06T686 and at Symmetricom and Draper Laboratory under Contract # NBCHC020050. The magnetometer work was supported by the US Army Corps of Engineers, at Sandia under MIPR number W74RDV60957676 and at Geometrics under contract W912HQ-06-C-0043. This work was also supported by Sandia, a multiprogram laboratory operated by Sandia Corporation, a Lockheed Martin Company, for the United States Department of Energy's National Nuclear Security Administration under contract DE-AC04-94AL85000.

REFERENCES

1. J. Kitching, S. Knappe, N. Vukicevic, L. Hollberg, R. Wynands, and W. Weidmann, "A Microwave Frequency Reference Based on VCSEL-Driven Dark Line Resonances in Cs Vapor," IEEE Trans. Instrum. Meas., vol. 49, pp. 1313–1317, 2000.
2. R. Lutwak, D. Emmons, W. Riley, and R.M. Garvey, "The Chip-Scale Atomic Clock – Coherent Population Trapping vs. Conventional Interrogation", Proceedings of the 34th Annual Precise Time and Time Interval (PTTI) Systems and Applications Meeting, December 3-5, 2002, Reston, VA, pp. 539-550.
3. D. K. Serkland, G. M. Peake, K. M. Geib, R. Lutwak, R. M. Garvey, M. Varghese, and M. Mescher, "VCSELs for atomic clocks," Proc. SPIE, vol. 6132, pp. 613208-1 to -11, 2006.
4. N. Cyr, M. Tetu, and M. Breton, "All-optical microwave frequency standard: A proposal," IEEE Trans. Instrum. Meas., vol. 42, pp. 640–649, 1993.
5. J. Vanier, A. Godone, and F. Levi, "Coherent population trapping in cesium: Dark lines and coherent microwave emission," Phys. Rev. A, vol. 58, pp. 2345–2358, 1998.
6. Y.-Y. Jau, E. Miron, A. B. Post, N. N. Kuzma, and W. Happer, "Push-Pull Optical Pumping of Pure Superposition States", Phys. Rev. Lett., vol. 93, p. 160802-1, 2004.
7. M Stähler, R. Wynands, S. Knappe, J. Kitching, L. Hollberg, A. Taichenachev, and V. Yudin, "Coherent population trapping resonances in thermal 85Rb vapor: D1 vs D2 line excitation," Optics Letters, vol. 27, pp. 1472-1474, 2002.
8. R. Lutwak, D. Emmons, T. English, W. Riley, A. Duwel, M. Varghese, D. K. Serkland, and G. M. Peake, "The Chip-Scale Atomic Clock – Recent Development Progress", Proceedings of the 35th Annual Precise Time and Time Interval (PTTI) Systems and Applications Meeting, December 2-4, 2003, San Diego, CA, pp. 467-478.
9. A. L. Bloom, "Principles of operation of the rubidium vapor magnetometer," Appl. Opt. 1, 61-68 (1962).
10. S. Groeger, G. Bison, J.-L. Schenker, R. Wynands, and A. Weis, "A high-sensitivity laser-pumped Mx magnetometer," Eur. Phys. J. D, vol. 38, pp. 239-247 (2006).
11. F. Monti di Sopra, H. P. Zappe, M. Moser, R. H¨ovel, H.-P. Gauggel, and K. Gulden, "Near-Infrared Vertical-Cavity Surface-Emitting Lasers with 3-MHz Linewidth", IEEE Photon. Technol. Lett., vol. 11, pp. 1533-1535, 1999.
12. R. Lutwak, P. Vlitas, M. Varghese, M. Mescher, D.K. Serkland, and G.M. Peake, "The MAC – A Miniature Atomic Clock", Proceedings 2005 Joint IEEE International Frequency Control Symposium and Precise Time and Time Interval (PTTI) Systems and Applications Meeting, Vancouver, BC, August 29-31, 2005.
13. D. L. Huffaker, D. G. Deppe, K. Kumar, and T. J. Rogers, "Native-oxide defined ring contact for low threshold vertical-cavity lasers,"Appl. Phys. Lett., vol. 65, p. 97, 1994.
14. D. K. Serkland, G. R. Hadley, K. D. Choquette, K. M. Geib, and A. A. Allerman, "Modal frequencies of vertical-cavity lasers determined by an effective-index model," Appl. Phys. Lett., vol. 77, pp. 22-24, 2000.
15. R. W. Herrick, "Oxide VCSEL reliability qualification at Agilent Technologies," Proc. SPIE, vol. 4649, pp. 130-141, 2002.
16. J. A. Tatum, A. Clark, J. K. Guenter, R. A. Hawthorne III, and R. H. Johnson, "Commercialization of Honeywell's VCSEL technology," Proc. SPIE, vol. 3946, pp. 2-13, 2000.